

# Optical influence of ship wakes

Xiaodong Zhang, Marlon Lewis, W. Paul Bissett, Bruce Johnson, and Dave Kohler

The optical variations observed within ship wakes are largely due to the generation of copious amounts of air bubbles in the upper ocean, a fraction of which accumulate as foam at the surface, where they release scavenged surfactants. Field experiments were conducted to test previous theoretical predictions of the variations in optical properties that result from bubble injection in the surface ocean. Variations in remote-sensing reflectance and size distribution of bubbles within the ship-wake zone were determined in three different optical water types: the clear equatorial Pacific Ocean, moderately turbid coastal waters, and very turbid coastal waters, the latter two of which were offshore of New Jersey. Bubbles introduced by moving vessels increased the backscattering in all cases, which in turn enhanced the reflectance over the entire visible and infrared wave bands. The elevated reflectance had different spectral characteristics in the three locations. The color of ship wakes appears greener in the open ocean, whereas little change in color was observed in near-coastal turbid waters, consistent with predictions. Colorless themselves, bubbles increase the reflected radiance and change the color of the ocean in a way that depends on the spectral backscattering and absorption of the undisturbed background waters. For remote observation from aircraft or satellite, the foam and added surfactants further enhance the reflectance to a degree dependent on the illumination and the viewing geometry. © 2004 Optical Society of America

OCIS codes: 010.4450, 290.1350, 280.0280.

## 1. Introduction

Waves and turbulence generated by a vessel moving in water result in a ship wake, which appears as a streak of foamy, turbulent water followed by a region of visually smooth water characterized by the absence of small-scale surface roughness. Moving ships create surface waves, also called Kelvin wakes,<sup>1</sup> and sometimes internal waves in the presence of a shallow pycnocline.<sup>2</sup> These wave patterns are also accompanied by copious quantities of bubbles created below the surface. Because of the nature of their surfaces, bubbles adsorb other particles and organic matter, which contribute to the accumulation of surfactant material that has been observed in the centerline wake.<sup>3</sup>

Ship wakes and their associated features have

been extensively studied. Both Kelvin wake waves and the centerline wake can effectively modify the Bragg scale waves, enabling ship wakes to be easily detected by microwave synthetic aperture radar observations.<sup>4</sup> Ship wakes have also been found to display a radiant intensity contrast in the thermal infrared.<sup>5</sup> Munk *et al.*<sup>6</sup> studied in detail how ship wakes produce a sun glitter pattern in optical images taken from the space shuttle. The acoustic effects of wake bubbles have been of great interest for a long time. There have been, however, few studies on the spectral variability of ship wakes in the visible and the near-infrared wavelengths.

There is emerging evidence that points to the significance of bubble populations to light scattering in the upper ocean.<sup>7,8</sup> From optical theory and limited field data on bubble populations, Zhang *et al.*<sup>7</sup> suggested that bubbles injected either by breaking waves or ship wakes increase the reflectance and change the color toward the green in the open ocean. Recently Stramski and Tegowski<sup>9</sup> analyzed the acoustic measurements of bubbles by breaking waves off the coast of Spitsbergen, Norway, and found that there could be significant bubble-induced changes in both the underwater light field of the surface layer and in the ocean reflectance and that the effect could vary drastically because of the intermittent nature of breaking waves. However, none of these studies have ad-

---

X. Zhang (zhang@aero.und.edu) is with the Earth System Science Institute, University of North Dakota, Grand Forks, North Dakota 58202-9007. M. Lewis and B. Johnson are with the Department of Oceanography, Dalhousie University, Halifax, Nova Scotia, Canada B3H 4J1. W. P. Bissett and D. Kohler are with the Florida Environmental Research Institute, 4807 Bayshore Boulevard, Suite 101, Tampa, Florida 33611.

Received 5 September 2003; revised manuscript received 24 February 2004; accepted 24 February 2004.

0003-6935/04/153122-11\$15.00/0

© 2004 Optical Society of America

dressed how the bubbles will modify light propagation in coastal, optically complex (case 2) waters,<sup>10</sup> and none involved direct measurement of the surface-reflectance variations that were due to bubble injection.

Our primary intention is to investigate how bubble populations in the upper surface layer will affect the color of the ocean of different water types. Here we focus on the optical influences of bubbles injected by moving vessels into the upper ocean. Bubbles produced in this way are in a more spatially confined state, the result of which, however, can be applied to the natural bubble population as well. We carried out direct hyperspectral-reflectance measurements within and outside of ship wakes in three different optical water regimes, one in the equatorial Pacific Ocean and the other two off the New Jersey coast. In addition, the bubble size distributions were also measured by photographic methods during the New Jersey experiments. The influence of bubbles in the surface layer on the hyperspectral reflectance of the ocean is discussed, along with a consideration of related changes that are due to turbulence, foam, or surfactant microlayers.

## 2. Background and Theoretical Bases

### A. Ship-Generated Bubbles

Breaking of bow waves and stern waves, both of which belong to the Kelvin wake system, produce bubbles.<sup>3</sup> Bubbles are also generated along the ship's hull as a result of air entrainment that is due to the frictional drag forces at the surface of the hull.<sup>11</sup> It has been postulated that the most copious source of bubbles in wakes, however, is propeller cavitation at high speed,<sup>11</sup> a hypothesis that to date, to our knowledge, has not been confirmed by field observations.<sup>12</sup>

Whereas Kelvin wakes radiate away from the ship with a half angle of 19.5° relative to the ship's bearing,<sup>1</sup> the newly generated bubbles are relatively confined within the centerline wake because of the horizontal converging wake flow behind the ship.<sup>1,3,4</sup> The centerline wake far behind a ship is accompanied by numerous persistent vortices, the center of which meanders along the direction of the ship track.<sup>13</sup> How these turbulent structures affect or regulate the distribution of wake bubbles has yet to be studied; however, field experiments have shown that bubbles will display a roughly homogeneous vertical distribution within the first several minutes<sup>12</sup> as a result of the strong turbulence created by the motion of the ship's hull and the action of its propellers and can reach down to several meters below the depth of the ship's bottom.<sup>14</sup> It has also been found<sup>12</sup> that the wake bubbles last as strong acoustic scatterers for approximately 7.5 min (~2 km astern for ship speed of 5 m s<sup>-1</sup> or 10 kn) with a maximum width of 60 m, although the surface-active film wakes have been observed to persist for tens of kilometers downstream of a surface ship.<sup>2,3</sup>

The gas-void fraction generated as bubbles by ship

wakes has been found to vary with ship size, propeller size, and rotation speed. The acoustic measurement of wake bubbles by a destroyer at 15 kn (~7.5 m s<sup>-1</sup>)<sup>11</sup> derived a concentration of approximately 6 × 10<sup>6</sup> m<sup>-3</sup> for bubbles between 80 and 1000 μm in radius. Based on analyses in Zhang *et al.*,<sup>7</sup> the minimum optical backscattering coefficient at 550 nm for this bubble population, assuming all with a radius of 80 μm, is between 0.0027 and 0.0097 m<sup>-1</sup>, depending on the thickness of their coatings. As a comparison, the typical particulate backscattering coefficient at the same wavelength as that in case 1 water<sup>10</sup> with a chlorophyll concentration of 0.1 mg m<sup>-3</sup> is only ~0.0007 m<sup>-1</sup>.<sup>15</sup> With the smaller bubbles taken into account, the contribution to the scattering by ship wakes will be even higher; it is clear that ship wakes can potentially significantly alter the backscattering of light in the upper ocean.

### B. Spectral Effects of Bubbles on the Reflectance

For an above-water observation, such as that from aircraft or satellite, the color of the ocean is often described by the spectral water-leaving reflectance, or the remote-sensing reflectance  $R_{rs}(\lambda) = \{[L_w(\lambda)]/[E_d^+(\lambda)]\}$ , where  $L_w$  is the water-leaving radiance at zenith and  $E_d^+$  is the downwelling irradiance just above the water. The variation of the spectral remote-sensing reflectance is linked to the inherent optical properties of the ocean, the total backscattering coefficient  $b_b(\lambda)$ , and the total absorption coefficient  $a(\lambda)$ , through<sup>10,16,17</sup>

$$R(\lambda) = \frac{E_u(\lambda)}{E_d^+(\lambda)} = f(\lambda) \frac{b_b(\lambda)}{a(\lambda)}, \quad (1a)$$

$$E_u(\lambda) = Q(\lambda) L_u(\lambda), \quad (1b)$$

$$R_{rs}(\lambda) = G \frac{f(\lambda) b_b(\lambda)}{Q(\lambda) a(\lambda)}, \quad (1c)$$

where  $Q$  is the ratio of upwelling irradiance  $E_u$  to the upwelling radiance at zenith  $L_u$  defined just below the surface and  $f$  is a dimensionless model parameter that numerically links the value of  $b_b/a$  to the diffuse reflectance  $R$ , which is defined as the ratio of upwelling irradiance  $E_u$  to the downwelling irradiance  $E_d$ , both of which are defined just below the surface. The parameter  $G$  accounts for cross-interface effects of propagating  $E_d^+$  to  $E_d$  and  $L_u$  to  $L_w$ . Its value changes <1% from 400 to 700 nm because of a slight variation in the refractive index of water with wavelength and can safely be considered as spectrally constant for practical applications.

For a given incident light field, the variations in the scattering and absorption properties of the ocean also modify the spectral values of  $f$  and  $Q$ .<sup>18,19</sup> However, studies for case 1 waters suggest that the ratio of  $f$  to  $Q$  is less variant and ranges between 0.08 and 0.12 in the visible for a wide range of conditions (0° ≤ solar angle ≤ 75°, 0.03 mg m<sup>-3</sup> ≤ chlorophyll concentration ≤ 10 mg m<sup>-3</sup>).<sup>16</sup> Therefore the spectral changes in the scattering and the absorption pro-

cesses can directly account for most of the variability in the color of the ocean observed from above.

Because the absorption by bubbles is negligible,<sup>7</sup> the injection of wake bubbles influences mainly the scattering. As a result, bubble injection increases the reflectance as

$$R_{rs,w}(\lambda) = G \frac{f_w(\lambda)}{Q_w(\lambda)} \frac{b_b(\lambda) + b_{b,bub}}{a(\lambda)}, \quad (2)$$

where  $b_{b,bub}$  is the backscattering coefficient for bubbles, which is spectrally flat because wake-bubble populations are dominated by large bubbles ( $>20 \mu\text{m}$ ),<sup>11,12</sup> and the changes of parameters  $f$  to  $f_w$  and  $Q$  to  $Q_w$  result from the changes in the volume scattering function of wake waters that are due to the injection of bubbles. Obviously two effects arise simultaneously as a result of bubble injections: The magnitude of reflectance increases with backscattering and the spectral distribution is changed.

From a similar analysis by Morel and Prieur for particles,<sup>10</sup> the spectral variation of ship wakes can be easily envisioned for open ocean regions, in which the dominant contribution to backscattering is that due to molecular scattering by seawater. The addition of bubbles in this case would proportionally enhance backscattering in the green and longer wavelengths, as the wavelength dependence of molecular scattering goes as  $\sim\lambda^{-4.3}$ .<sup>20</sup> Therefore the brighter and greener ship wakes that are often observed are due to the added backscattering by injected bubbles and its ensuing effect on flattening of the spectral peak of background water reflectance toward longer wavelengths. Because of the strong absorption by water molecules in the red wavelengths, most of the variation in the color of the ocean is restricted to the blue–green part of the spectrum. An approximate estimate of the color can be gauged by the formation of a blue–green reflectance ratio,  $\rho_{440-550} = \{[R_{rs}(440)]/[R_{rs}(550)]\}$ .

### C. Increased Reflectance between 750 and 800 nm

In a highly absorbing medium, such as in the infrared domain for water, the scattering process is dominated by single scattering. Zhang<sup>21</sup> simulated the hyperspectral reflectance as a result of bubble injection for various bubble concentrations and found that the increased reflectance in the longer wavelengths ( $>600 \text{ nm}$ ) in bubbly water is due effectively to bubbles alone and does not depend on the concentration of other particulates that may exist. Between 750 and 800 nm, in which the absorption by water molecules does not change very much ( $\sim 2.2\text{--}2.5 \text{ m}^{-1}$ ), we can derive a relationship linking the increased reflectance with the bubble concentration as

$$\Delta R_{rs}(750 \leq \lambda \leq 800) = R_{rs,w} - R_{rs} = 2.8 \times 10^{-11} N_0, \quad (3)$$

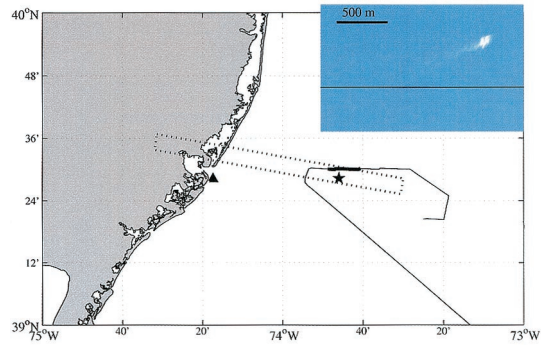


Fig. 1. Experiment sites for the Coast Wake. The triangle indicates the location for the Near Coast Wake on 28 July 2000, and the star for the Far Coast Wake on 31 July 2001, when the hyperspectral sensor PHILLS-2 was imaging the area surrounded by dotted lines. The inset displays a portion of the imagery showing the ship and wakes in true color composite. The solid line is the ship track for R/V Endeavor, which took surface measurements on 30 July 2001.

where  $N_0$  (in inverse cubic meters) is the concentration of bubbles at the surface,  $R_{rs}$  is the “background” reflectance of the undisturbed sea, and  $R_{rs,w}$  is the reflectance of the water with additional bubbles added. Note that Eq. (3) is based on the calculations for wind-generated bubbles, and we apply it here to wake bubbles, assuming that the bubble size distribution produced by the two events are similar (see Subsection 4.B and Fig. 5). Note as well that, in principle, the reflectance outside of the wake could also include the influence of bubbles as a background population introduced by breaking waves or biological activity; for this analysis, we assume that their influence is small compared with that of the bubbles injected by a moving vessel.

### 3. Methodology

We evaluated the optical variation induced by ship wakes from two perspectives, model simulations and field measurements. We conducted field experiments in three different optical water regimes. The first was in the western equatorial Pacific Ocean onboard the research vessel Mirai (Japan Marine Science and Technology Center), from December 1998 to January 1999. The second (July 28, 2000) and third (July 31, 2001) experiments took place in coastal waters off New Jersey (Fig. 1),<sup>22</sup> in association with the Hyperspectral Coastal Ocean Dynamics Experiment at the LEO-15 area offshore of New Jersey (LEO is the Longterm Ecosystem Observatory, Rutgers University). The experiment site in 2000 (indicated by the filled triangle in Fig. 1) was very close to the coast, whereas in the 2001 experiment, the ship was moving in an area offshore (indicated by the filled star in Fig. 1). We refer to the experiment in the equatorial Pacific as Ocean Wake and those at the LEO-15 as Near Coast Wake and Far Coast Wake.

### A. Ocean Wake Experiment

In the Ocean Wake experiment, the mean chlorophyll-a concentration, as measured aboard ship, was  $<0.1 \text{ mg m}^{-3}$  for the region during the time, and the background attenuation coefficient ( $c = a + b$ ) at 490 nm was  $\sim 0.03 \text{ m}^{-1}$ . Measurements of upwelling radiance and downwelling irradiance near the sea surface were made with the hyperspectral tethered spectral radiometer buoy (TSRB; Satlantic Inc.). The TSRB measures the upwelling hyperspectral radiance at a depth of 0.6 m and downwelling irradiance just above the surface from 400 to 800 nm with a spectral resolution of 3.3 nm and a frequency of 1 Hz. The ratio of the upwelling radiance to the downwelling irradiance, both of which are propagated to just above the sea surface, forms the remote-sensing reflectance as defined above.

The TSRB propagation method involves the uses of two empirical models by Austin and Petzold<sup>23</sup> and Morel<sup>24</sup> for wavelengths between 400 and 700 nm. For wavelengths above 700 nm, only the attenuation that is due to water molecules is corrected for. Zhang<sup>21</sup> evaluated the TSRB propagation algorithm performance in both clear and bubbly waters. The TSRB algorithm works well for case 1 waters, except for the spectral band between 650 and 700 nm, in which the influence by phytoplankton fluorescence and Raman scattering causes overestimates of  $<15\%$  in the upwelling radiance just below the surface. On the other hand, the presence of bubbles causes an underestimate of the upwelling radiance. This is because the band-ratio algorithm used is not very sensitive to scattering by bubbles, which, however, increase the attenuation by increasing scattering over the entire spectrum. However, because of the short propagation distance (0.6 m), the errors are generally less than 20% and less than 10% for the blue and the green wavelengths. In this study, we used the standard TSRB algorithm to estimate the reflectance at the surface for both background and wake-zone waters.

The measurements were first taken under calm seas behind the ship, which had stopped for a long period. The propeller was then run briefly (5 s) at high speed to generate cavitation bubbles. The TSRB was then situated in the resulting bubble cloud and allowed to stream with the cloud as it was advected away from the ship. Each measurement series, for both background control and bubble injection, was taken for 3 min ( $\sim 90$  records), and the result used in this study is the median record. The median estimate reduces the potential contamination from foam and other environmental variance.

### B. Near Coast Wake Experiment

In the Near Coast Wake experiment, the water was very turbid because of runoff from the adjacent marsh and wetlands, with an average attenuation coefficient  $c$  (490 nm) of  $>3 \text{ m}^{-1}$ . The ship wakes were generated by a small outboard motorboat, which was driven across the experiment site. Measure-

ments were taken from an instrumented catamaran, which was towed over the wakes. Measurements were made of upwelling hyperspectral radiance at a depth of 0.6 m and of downwelling irradiance above the surface as in the equatorial experiment with a TSRB fixed to the catamaran. An underwater bubble camera provided imagery of the bubble population. At each wake crossover, the TSRB was turned on for 5 min and the camera took pictures every 45 s.

The camera system is an improved version of a previous instrument<sup>25</sup> and is designed to measure the number density of bubbles over a large size range by use of a high-resolution digital camera. Based on laboratory calibrations, the resolution of the camera is  $19 \text{ }\mu\text{m}/\text{pixel}$  and therefore the minimum size of a bubble that could be resolved by the camera is  $\sim 40 \text{ }\mu\text{m}$  (at least two pixels are needed to identify a bubble).

### C. Far Coast Wake Experiment

In the Far Coast Wake experiment, an airborne hyperspectral imaging sensor (Portable Hyperspectral Imager for Low Light Spectroscopy, version 2, or PHILLS-2) was deployed over the LEO-15 site and imaged a passing ship that had produced a long wake in the field of view (Fig. 1). The aircraft was flown at 9 km; given the instantaneous field of view of the sensor, this results in a ground resolution of approximately  $9 \times 9 \text{ m}/\text{pixel}$  from 404 to 964 nm. The radiance recorded by PHILLS-2 was normalized by the downwelling irradiance measured at the sea surface by the TSRB onboard R/V Endeavor (0.5 h later) to generate the reflectance, which is in a reduced spectral range from 400 to 800 nm as limited by the TSRB wavelengths. The reflectance thus computed will be slightly lower than what would be measured in the wake, because the downwelling irradiance will be higher half an hour later in the morning. We estimated the changes in the solar flux by using MODTRAN<sup>26</sup> with the typical atmosphere gas and aerosol profiles that are applicable to the experiment, and found that the error will be  $\sim 10\%$  in the blue and lower in the longer wavelengths (result not shown).

The PHILLS-2 data we used were not atmospherically corrected, which will introduce uncertainties in three aspects: The first is due to the attenuation of the water-leaving radiance by the atmospheric gases and aerosols; the second is due to scattered light along the atmospheric path length; and the third is due to the variation of the path length from the center to the edges of the image (sensor views a  $\sim 17^\circ$  half angle). For an atmosphere with a nonabsorbing aerosol, the atmospheric attenuation of the water leaving radiance from the surface to the sensor 9 km above is dominated by Rayleigh scattering<sup>27</sup> and ranges from 0.90 to 0.99 for wavelengths from 400 to 800 nm. It may be lower if the aerosol is absorbing. The atmospheric path length is  $\sim 5\%$  greater on the edges of the image versus the nadir view; however, for the area of interest surrounding the ship, which is located close to nadir, the path-length variation is  $<2\%$  (approximately 1/3 of the half-angle view).

Given such a small variation of atmospheric path length, the atmospheric contributions do not change significantly within the wake zone, and their effect is canceled out in the difference of reflectance between ship wakes and the background waters, with a maximum error of  $\sim 10\%$  in the blue that is due to the beam attenuation.

The day before the wake experiment, surface measurements covering the same area (thin line in Fig. 1) were conducted onboard R/V Endeavor. The average beam attenuation coefficient  $c$  (490 nm) along the thick line in Fig. 1 was  $1.62 \text{ m}^{-1}$ . It was windy for two days before the experiment and relatively calm during the experiment with an average wind speed of  $\sim 6\text{--}7 \text{ m s}^{-1}$ .

Even though the wake system defines a wider spatial extent in general, in what follows we use the term “(ship) wakes” to refer to water immediately behind a ship or in the centerline wake along the ship track, within which high concentrations of bubbles are found.

#### D. Model Simulations

We used an advanced in-water radiative transfer model, HydroLight,<sup>28</sup> to verify further the role played by wake bubbles in modifying the spectral variation of reflectance observed in ship-wake zones in different waters.

In the model, only bubbles are assumed to be introduced by ship wakes. The background waters are assumed to be case 1, and their optical properties are calculated with models built into HydroLight for the absorption,<sup>29</sup> scattering,<sup>30</sup> and phase function<sup>31</sup> for these water types. During the Ocean Wake experiment, the chlorophyll concentration is measured at  $0.1 \text{ mg m}^{-3}$  for the surface water and a deep chlorophyll maximum of  $0.5 \text{ mg m}^{-3}$  is assumed to be located at 50 m depth.<sup>32</sup> For the Far Coast Wake experiment, a constant chlorophyll concentration of  $3 \text{ mg m}^{-3}$  is assumed to a depth of 40 m.<sup>22</sup> The assumption of case 1 water type obviously does not apply to the Near Coast experiment site (indicated by the filled triangle in Fig. 1), for which, however, we do not have sufficient knowledge of the inherent optical properties either. To examine how this uncertainty affects our results, we simply use the same case 1 models for this site and assume a chlorophyll concentration of  $10 \text{ mg m}^{-3}$  down to a 10-m depth. The models we choose to use are not meant to reproduce the exact optical characteristics of the field; rather they are used to define an approximate background state, against which we are interested in the reflectance enhancement only as a result of injected bubbles by ship wakes. For example, the model gives a total attenuation coefficient at 490 nm of  $1.32 \text{ m}^{-1}$  for the Far Coast Wake, compared with the ship determination of  $1.62 \text{ m}^{-1}$ .

For all the simulations, the phase function is calculated for bubbles of sizes between 1 and  $300 \text{ }\mu\text{m}$  with a protein coating of  $0.1 \text{ }\mu\text{m}$  thick,<sup>33</sup> and the mean scattering cross-sectional area is  $3.6 \times 10^{-8} \text{ m}^2$ , a value representative of wind-generated bubble

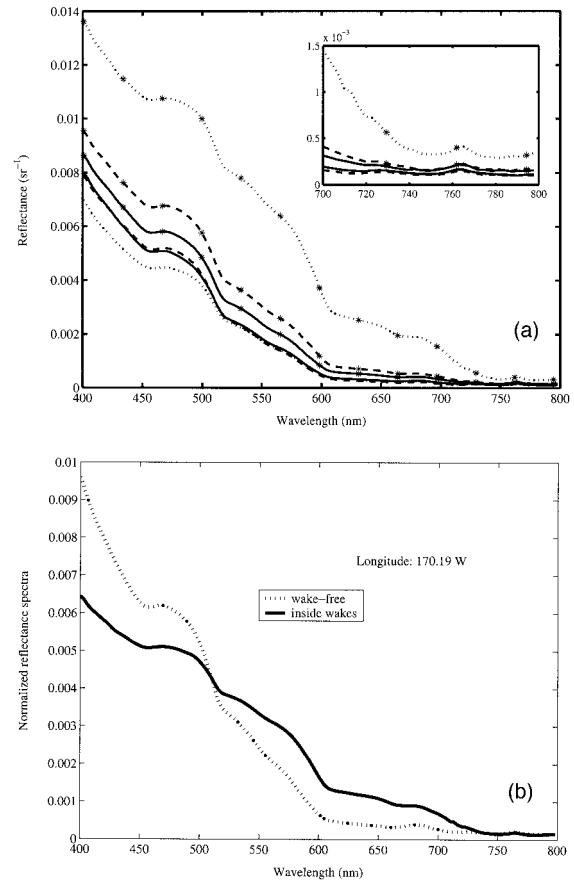


Fig. 2. (a) Comparison of measured reflectance between the inside (curve with stars) and the outside (plain curve) of the wake zone at three stations along the equator during the Ocean Wake experiment [from West to East, 163.60 E (solid curve), 176.30 W (dashed curve), and 170.19 W (dotted curve)]. The inset is an enlarged view of the measurements between 700 and 800 nm. (b) Shape of the measured reflectance spectra at the St. 170.19 W normalized by the corresponding integral over the waveband 400–800 nm.

populations.<sup>21</sup> The bubbles are assumed to be distributed uniformly in the top 1 m. The bubble concentration is determined from Eq. (3) with *in situ* measurements of the increased reflectance.

## 4. Results

### A. Ocean Wake Experiment

The reflectance measured at three stations along the equator, 163.60E, 176.30W, and 170.19W, during the Ocean Wake experiment are shown in Fig. 2(a). Clearly the reflectance inside the wake is elevated over the entire visible spectrum against the background state, in agreement with the prediction of Eq. (2). The increased reflectance, albeit slightly, was observed in the near infrared as well [Fig. 2(a), inset]. Note also that the reflectance enhancement between 750 and 800 nm is relatively uniform, consistent with what we found for the wind-generated bubble populations (Subsection 2.C). The reflectance spectra for all of the wake-free waters are similar, which is typ-

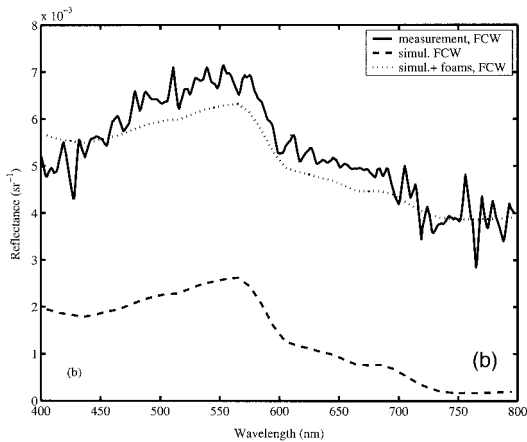
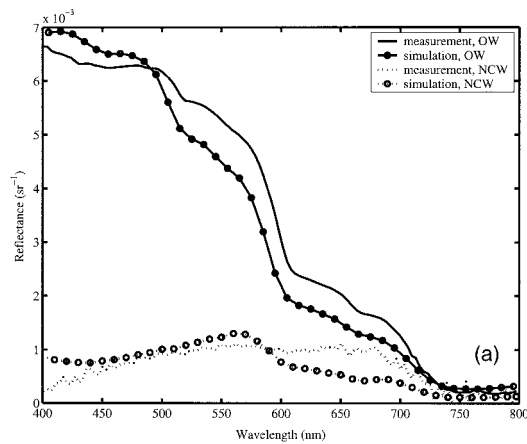


Fig. 3. Comparison of the increased reflectance between the measurements and the model simulations for (a) St. 170.19 W of the Ocean Wake (OW) and the Near Coast Wake experiments and (b) for the Far Coast Wake (FCW) at 500 m behind the ship.

ical for this region where the optical properties do not change very much in the surface layer. It varied inside the wakes for different stations, probably because of variations in the concentration of bubbles generated by the propeller of the vessel.

From west to east (i.e., in the following order: 163.3E, 176.E, 170.19W), the blue-green ratios,  $\rho_{440-550}$ , of the background water were 3.09, 3.28, and 2.79, and they decreased to 2.67, 2.42, and 1.60, respectively, in the wake. The spectral distribution of the reflectance also changed in the wake zones. An example of the spectral change is shown in Fig. 2(b), in which the reflectance spectrum for both background and wake waters measured at station 170.2°W is normalized to its integrated value over the entire spectrum. Clearly the steepness of the background spectrum that strongly favored blue wavelengths is flattened by the introduction of bubbles, and relatively more light from green and longer wavelengths contributes to the reflectance spectrum.

Using Eq. (3), we estimated that the enhanced bubble concentrations at the three stations, from west to east, were  $1.6 \times 10^6$ ,  $2.2 \times 10^6$ , and  $7.4 \times 10^6 \text{ m}^{-3}$ , respectively. The concentrations are comparable with the wake-bubble density of  $6 \times 10^6 \text{ m}^{-3}$  mea-

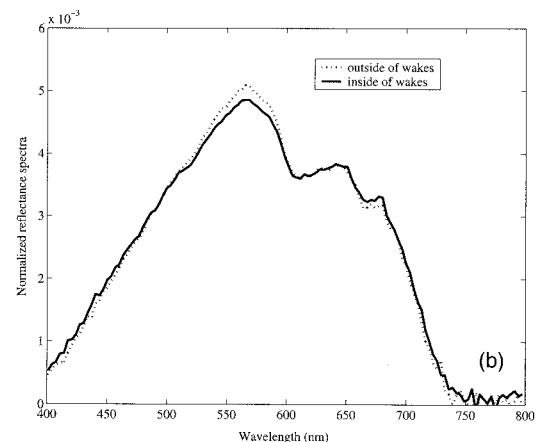
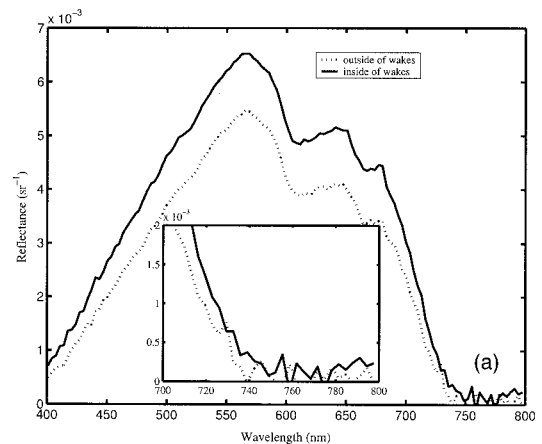


Fig. 4. Same as Fig. 2 except for the Near Coast Wake experiment. In both Figs. 3(a) and 3(b), the solid curve is for measurement inside the wake, and the dotted curves for measurements taken outside.

sured acoustically for a destroyer at 15 kn.<sup>11</sup> Figure 3(a) shows the comparison of reflectance enhancement between measurement (solid curve) and model results (solid curve with circles) for the station at 170.19W with an estimated wake-bubble concentration of  $7.4 \times 10^6 \text{ m}^{-3}$ . The variations in the reflectance observed in the Ocean Wake experiment are largely reproduced by the model prediction. The deviations (<15%) found in the visible wavelengths are partly due to errors associated with defining the initial state of the absorption and the scattering. The absorption errors are almost completely inherited in the reflectance difference, whereas the scattering errors are only partially canceled out because of the multiple-scattering effects between bubbles and the unaccounted particles.

#### B. Near Coast Wake Experiment

The reflectances measured outside and inside wakes during one wake crossing are shown in Figure 4(a). The amplitude of the background reflectance for wavelengths below 500 nm is smaller than that measured during the Ocean Wake experiment because of the presence of high concentrations of absorbing materials, such as phytoplankton and dissolved organic

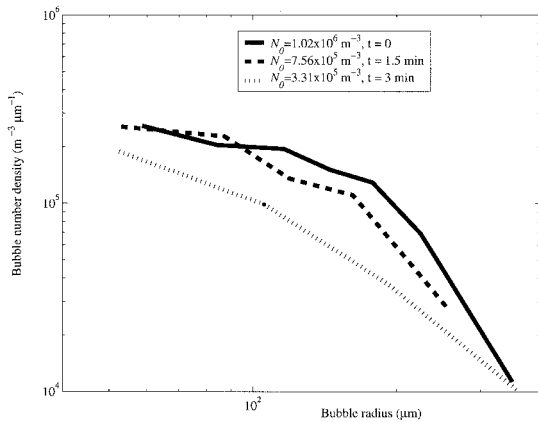


Fig. 5. Size distributions of ship wake bubbles determined by the underwater camera during the Near Coast Wake experiment, and their variation with time.  $N_0$  in the legend denotes the total number density of bubbles that could be resolved by the camera.

material; the opposite is true for the longer wavelengths because of strong scattering by high concentrations of suspended particles. The reflectance is dominated by a green–yellow signal (550–600 nm); the shoulder between 600 and 650 nm is likely related to brownish particulates suspended in the coastal water. The fluorescence peak at 680 nm is clearly visible, suggesting a high concentration of phytoplankton pigment. Despite the significant differences in the background spectral signatures between the Near Coast and the Ocean Wake experiment sites, the general optical effect of the ship wakes is the same, i.e., the reflectance increases over the entire spectrum. Note that the measurements were noisy between 750 and 800 nm, probably because of the high turbidity of the water. Despite that, the reflectance between 750 and 800 nm is relatively constant for both background and wake waters, and the reflectance enhancement is approximately  $1 \times 10^{-4} \text{ sr}^{-1}$ , which translates into a bubble concentration of  $3.7 \times 10^6 \text{ m}^{-3}$  [Eq. (3)].

Contrary to the observation of a decrease in the blue–green ratio in the Ocean Wake experiment,  $\rho_{440-550}$  increased slightly from 0.338 outside of the wakes to 0.380 inside the wakes and the water within the wake in the Near Coast became less green than before [Fig. 4(b)]. However, the spectral variation in the Near Coast Wakes is small compared with that found in the open ocean, and visually there is little difference in the color of the sea in the wake zone, except in foam patches.

Three sequential (90-s intervals) size spectra of ship-wake bubbles, derived from the underwater camera measurements during the same crossing, are shown in Figure 5. The size range of bubbles that could be identified is between 40 and 400  $\mu\text{m}$ . The initial size spectrum outside of the wake showed a slope of  $< -1$  for bubbles less than 120  $\mu\text{m}$  and  $-4$  for larger bubbles. This size variation agrees with theoretical predictions<sup>34</sup> and with field observations for wind-generated bubbles,<sup>35,36</sup> although the slope for

the smaller part of the size spectrum is somewhat smaller. The size spectrum assumes a less variable slope of  $-1.5$ – $-2.5$  3 min later. The total number of bubbles within this size range decays with time, from approximately  $1 \times 10^6 \text{ m}^{-3}$  initially to  $3 \times 10^5 \text{ m}^{-3}$  after 3 min. These numbers are slightly lower than the value of  $3.7 \times 10^6 \text{ m}^{-3}$  estimated directly from the reflectance by use of Eq. (3). This is because the camera was not able to identify bubbles that attach to particles that are present in high concentrations and because the camera cannot resolve smaller bubbles, which also exist in large numbers. Therefore the figures provide a lower bound on the actual bubble density created by the ship wakes.

By use of the bubble concentration derived from the reflectance measurement, the model gave a better comparison with the measurement in general, and the results are shown in Fig. 3(a) (dotted curves with and without circles). Bubbles account for most of the optical variations that are observed in this very turbid coastal water. Relatively large errors found between 600 and 700 nm (corresponding to the shoulder in Fig. 4) are probably due to multiple-scattering effects between bubbles and nonphytoplankton particles, the latter of which are not included in the model we used.

### C. Far Coast Wake Experiment

A series of points along the ship track was chosen and the corresponding reflectances estimated from the PHILLS-2 imagery [Fig. 6(a)]. Compared with Fig. 2(a) and 4(a), which are based on direct surface measurements, the reflectance measured from the aircraft in the coastal waters off New Jersey shows a significant increase in the magnitude for the entire spectrum and a stronger relative weighting of the spectra in the blue. Both effects are due to strong contributions by atmospheric scattering and direct specular reflection of skylight. The reflectance for the wake waters, however, is higher than that of the background water, with magnitudes decreasing away from the ship along the centerline of the wake. The reflectance spectra of the background waters show little variation ( $< 2\%$ ) in terms of their magnitude and spectral shape, which supports our assumption that uncertainties that are due to variation of the atmospheric path length within the wake zone have a limited effect on the measured spectral radiance. Shown in Fig. 6(a) (the bottom solid curve) is a representative spectrum of the background water (including atmospheric scattering and surface specular reflection contributions).

Because of the strong influence of the atmospheric scattering on the airborne measurement of the wake reflectance, we have to remove the atmospheric effect before evaluating the spectral variation in the Far Coast Wake experiment. Figure 6(b) shows the difference in the reflectance spectra between the wake water and the background water. The wake waters over 1.2 km behind the ship are almost indistinguishable from the surrounding waters in terms of surface reflectance. Wake waters closer to the ship ( $< 500$

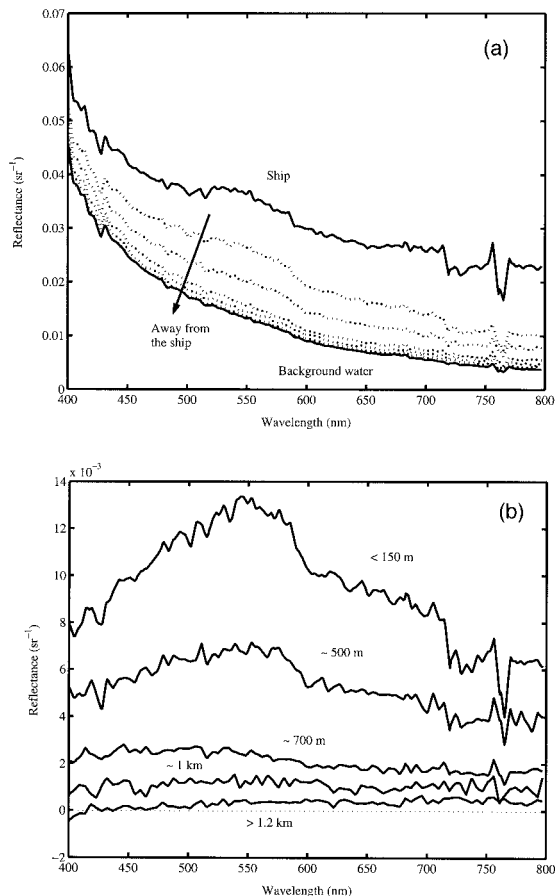


Fig. 6. (a) Hyperspectral reflectance derived from the airborne sensor PHILLS-2 for the ship, background water, and wake water. From top to bottom, the reflectance within the ship wakes (dotted curve) was sampled at an increasing distance away from the ship. (b) The increased reflectance of ship wakes against the background water. The numbers shown are the distance from the ship at which the reflectance spectrum is estimated.

m) show enhanced reflectance in the green wavelengths, whereas wake waters farther away show a more or less uniform increase. As already pointed out, the atmospheric contribution to the measured reflectance is largely canceled out in the difference spectrum. However, a visual comparison for the wavelengths 750–800 nm between Fig. 6(b) and Fig. 3(a) indicates high reflectance values. For example, 500 m behind the ship, the reflectance enhancement in this infrared band is more than an order of magnitude higher than the measurements in the other two sites.

We therefore make several assumptions to estimate the bubble concentration for the Far Coast Wake: first, that the initial concentration of bubbles in the Far Coast Wake is the same as that in the Ocean Wake ( $7.4 \times 10^6 \text{ m}^{-3}$ ); second, that the bubble concentration decays at the same rate as in the Near Coast Wake (losing 25% after 1.5 min and 70% after 3 min; see Fig. 5); and third, that the vessel velocity is 15 kn ( $\sim 7.5 \text{ m s}^{-1}$ ). The bubble concentration thus derived 500 m behind the ship is approximately

$6.5 \times 10^6 \text{ m}^{-3}$ . The increased reflectance calculated from the model [dashed curve of Fig. 3(b)] was compared with the measurement [solid curve of Fig. 3(b)]. Although there is a shift in the overall magnitude between the two curves, the general spectral variations are similar. For example, both model and observation show a slow increase of reflectance from 400 to 550 nm, a quick decrease from 550 to 600 nm, a slow decrease again from 600 to 750 nm, and little change between 750 and 800 nm.

## 5. Discussion

The *in situ* observations in both the open ocean and the coastal waters have shown that optical reflectance is enhanced in waters inside ship wakes across the entire visible and near-infrared portion of the spectrum. Waters showing increased reflectance are contained within the centerline wake, even though wake waves spread over a much wider range. Given the assumption that only bubbles are introduced in ship wakes, the model predictions compared well with field measurements of the increased reflectance. This suggests that bubbles account for most of the optical variability that can be observed in the wake zone.

The color change, however, is different for various water regimes. In the Ocean Wake experiment, the wake water is greener than the background water [Fig. 2(b)], whereas in the Near Coast Wake experiment, there is very little change in the color of the sea [Fig. 4(b)]. Colorless themselves, bubbles can modify the color of the ocean only through the scattering process; after being injected into the ocean, bubbles increase the scattering, especially in the backward directions, equally across the entire visible and near-infrared spectra. The net effect is to enhance and flatten out the backscattering spectrum. In a turbid region, such as the Near Coast Wake site, the particle concentration, especially of large particles, is very high, and the backscattering spectrum is normally flat,<sup>15</sup> and there would be little change in the backscattering spectrum. The resulting color change is also modulated by the absorption spectrum [Eq. (2)]. The greener wake water observed in the open ocean is partly due to the absorption minimum in the shorter wavelengths as the chlorophyll, and the colored dissolved organic matter (CDOM) concentrations are low. However, if there is a strong absorption in the shorter wavelengths, say, in the presence of a high concentration of CDOM, the broadening of the backscattering spectrum into the green will be significantly neutralized by the strong absorption of CDOM. As a result, ship wakes will show little change in the color in this type of water, such as might be found in a clear lake.

Although bubbles can explain most of the spectral variability in the reflectance as observed in a wake zone by an *in-water* measurement, there are other factors that also potentially contribute to reflectance changes recorded from an above-water observation [Fig. 3(b)]. If the incident light field remains the same, the factors other than bubbles that are intro-

duced by ship wakes and that can also possibly affect the reflectance spectrum include turbulence, changes in the surface roughness, and formation of foam resulting from bubbles bursting at the surface. Turbulence can potentially affect light scattering in the upper water layer that can be observed from both above-water and in-water measurements,<sup>37</sup> wake waves have been found to increase the probabilities of sun glitter by enhancing the dynamic angular range of surface capillary waves,<sup>6</sup> and foam will also increase the reflectance across the entire spectrum.<sup>38</sup>

#### A. Effect of Turbulence-Induced Scattering

Ship wakes also produce, in addition to bubbles, turbulence, which in turn will cause small disturbances of the refractive index on the microscale. These small-scale variations in the refractive index will primarily modify the volume scattering function at the near-forward angle and hence increase the scattering magnitude; however, the effect is largely limited to very small angles ( $<0.1^\circ$ ).<sup>37</sup> Gordon<sup>39</sup> showed that the upwelling radiance could be estimated with an error of less than 5% if the uncertainty in the small-angle scattering is limited to within  $15^\circ$ . Therefore we expect that the wake turbulence-induced scattering has a maximum influence on the measured reflectance of less than 5% within the ship wakes. The uncertainty associated with turbulent scattering might account for some difference of Fig. 3(a), but its magnitude is too small to explain the discrepancy found in Fig. 3(b).

#### B. Effect of Surface Roughness

Ship wakes also introduce added surfactants, resulting in reduced surface roughness that will affect observations from above water. Mobley<sup>40</sup> found that roughened surfaces tend to reflect more direct sunlight and skylight into an above-water sensor than calm surfaces (depending on the viewing-illumination geometry), which results in changes in both the magnitude and the spectrum of the measured surface reflectance above the water. The turbulence generated by a moving ship is located immediately surrounding the ship<sup>4</sup> and diminishes very quickly away from the ship. Wake waves can also increase the roughness and can extend far astern. Munk *et al.*<sup>6</sup> interpreted the V-like wakes behind surface ships revealed in optical images from a space shuttle in terms of sun glitter from the tilted facets of a Kelvin wake. These V-like glitter patterns, however, have a very wide angle ( $>19.5^\circ$ ) with respect to the ship's velocity vector. The wake area, which shows increased reflectance in our analysis, is located in the centerline wake, which tends to have reduced surface roughness that is due to the damping effect of organic films released by bubbles as they break at the surface.<sup>3</sup>

The Far Coast Wake experiment took place at approximately 9:30 a.m. local time with a sun zenith angle of  $\sim 50^\circ$  and a relative azimuth angle of  $\sim 94^\circ$  between the viewing plane and the solar plane. Thus only wake facets with a tilt between  $25^\circ$  and

$27.5^\circ$  from the vertical and an azimuth orientation of  $\sim 47^\circ$  relative to the Sun can potentially produce sun glitter in the PHILLS-2 sensor with a half-angle view of  $17^\circ$ .<sup>41</sup> Given the wind speed of  $\sim 6 \text{ m s}^{-1}$  at the time when the PHILLS-2 passed the site, the probability for the capillary wave facets to have a tilt as high as  $25^\circ$  is  $\sim 1.5\%$ .<sup>42</sup> Because the small-scale roughness in the centerline wake will be significantly reduced by the presence of accumulated surfactant material released by bursting bubbles, we expect the probability to be even lower than 1.5%. For the more difficult problem of sky glitter, we would need to convolute the full sky radiance distribution with a statistical description of the surface slope variance for a complete solution. However, given that the Fresnel reflectance coefficient varies only weakly for angles of less than  $30^\circ$  or so, and given the particular conditions experienced here (weak winds and clear skies, viewing angle close to nadir and normal to the Sun's plane) it is unlikely that the observed increases in reflectance would result from changes in surface roughness.

#### C. Effect of Foam

Foam is generated by moving ships and forms the edge of the centerline wake zone. Bubbles that float to the surface but do not break also contribute to foam formation. For each pixel of the PHILLS-2 sensor, this foam also contributes to the above-water measurement, weighted by the fractional foam coverage in the area of each pixel. Relative to the background reflectance, the sensor measured a reflectance enhancement [solid curve of Fig. 3(b)] as

$$\begin{aligned} \Delta R_{rs} &= W(R_{rs,f} - R_{rs}) + (1 - W)(R_{rs,w} - R_{rs}) \\ &\approx WR_{rs,f} + R_{rs,w} - R_{rs}, \end{aligned} \quad (4)$$

where  $W$  is the fractional coverage of foam, and the subscripts  $f$  and  $w$  indicate foam and wake, respectively. The approximation takes place because we have assumed that the foam reflectance is much higher than the reflectance of foam-free waters. Note that the atmospheric contribution is assumed to be canceled out in Eq. (4).

From Fig. 3(b), we have  $\Delta R_{rs}$  (solid curve) and  $R_{rs,w} - R_{rs}$  (dashed curve) the term  $WR_{rs,f}$  of Eq. (4), the weighted contribution by foam to the measured reflectance, accounts for the difference between the two curves. Because our estimate of  $R_{rs,w} - R_{rs}$  is based on assumptions regarding the optical properties of the background water and the bubble concentration, there are unknown errors in the calculation. However, the error is well constrained in the spectral range between 750 and 800 nm because reflectance is small even for bubbly water. For example, a 100% uncertainty in this band would incur only a 5% error for the estimate of  $WR_{rs,f}$ , whereas the same amount of uncertainty of  $R_{rs,w} - R_{rs}$  in the green bands would cause a 40% error in  $WR_{rs,f}$ .  $WR_{rs,f}$  thus determined for the wavelengths between 750 and 800 nm is  $\sim 0.0037 \text{ sr}^{-1}$ . Assuming a neutral spectrum for the

foam reflectance,<sup>43,44</sup> we reconstructed  $\Delta R_{rs}$  by using Eq. (4), which is shown as a dotted curve in Fig. 3(b).

The comparison of the reconstructed  $\Delta R_{rs}$  with the measurement suggests that we have largely restored the magnitude of measured reflectance in the wake zone by taking foam into account. We also note that the reconstructed  $\Delta R_{rs}$  is systematically lower than the measurement in the wavelengths between 450 and 700 nm. This is probably due to our assumption of a white reflectance spectrum for the wake foam. Recently, field measurements of wind-generated foam have shown that foam actually reflects more in the visible than in the near-infrared wavelengths.<sup>38,45</sup> A better agreement can be achieved if we use a 15% higher foam reflectance in the visible (result not shown); the value is somewhat lower than the measured foam-reflectance spectrum both in the open ocean (20%)<sup>45</sup> and in the surf zone (30%–35%).<sup>38</sup> Obviously, if we know  $R_{rs,f}$ , we can easily estimate the foam coverage  $W$ . Given the wide range of values of  $R_{rs,f}$  that have been reported, the foam coverage estimated (500 m behind the ship) varies between 5% and 20%.

## 6. Conclusions

Field observations of hyperspectral reflectance have revealed that ship wakes change the ocean remote-sensing reflectance in both the magnitude and in the spectral shape. Using an advanced radiative transfer model, we confirmed that bubbles produced in ship wakes can account for most of these variations, either directly or as contributions from foam and scavenged surfactants. The wake foam also shows reduced reflectance toward infrared wavelengths, which is consistent with previous measurements for whitecaps. Turbulence and changes in the surface roughness, both of which are also introduced by ship wakes, have a minimal impact on the measured reflectance within the wake zones in the particular cases investigated. Note, however, that, under favorable viewing geometry, the smooth centerline wake can produce variations in specular sun glitter and changes in apparent sky reflectance for a remote sensor.<sup>6</sup>

The injection of wake bubbles, although colorless themselves, increases the scattering equally across the entire spectrum and can potentially change the color of water in the ship-wake zone. The color shift is most evident in the open ocean, where the weak absorption in the shorter wavelengths helps accentuate the broadening of the backscattering spectrum; consequently wakes appear greener. In turbid water, as the concentration of particulates increases the backscattering spectrum in a more spectrally neutral way, bubbles have less effect on changing the color of the sea. The amplitude of the reflectance is enhanced, but ship wakes show little color change in turbid waters.

These optical influences in the wake zone will decay with time. The measurements of the size spectra of wake bubbles suggest that only 30% of the population remain after 3 min. The remaining bub-

bles, however, can still produce a distinctive hyperspectral signature, which can be resolved for  $\sim 1$  km behind the ship in the coastal waters.

The wake bubbles are in a more or less spatially confined region astern of moving vessels at sea. The optical influences of bubbles injected by surface ships can be extended to natural bubble populations, which have a much larger spatial extent and can therefore potentially affect satellite and aircraft observations of the color of the sea. As shown in Figs. 2(a), 4(a), and 6(b), the enhanced scattering of bubbles will increase the reflectance over both the visible and the near-infrared wavelengths and invalidate the black pixel assumptions<sup>46</sup> used in routine atmospheric correction for ocean color remote sensing. The application of many case I water bio-optical algorithms will fail in the presence of significant bubbles as the chlorophyll concentration will be overestimated because of the misinterpretation of the green shift in the spectral reflection caused by the injection of bubbles into the upper ocean.

## References

1. L. Debnath, *Nonlinear Water Waves* (Academic, Boston, 1994), p. 544.
2. J. D. Lyden, R. R. Hammond, D. R. Lyzenga, and R. A. Shuchman, "Synthetic aperture radar imaging of surface ship wakes," *J. Geophys. Res.* **93**(C10), 12293–12303 (1988).
3. R. D. Peltzer, O. M. Griffin, W. R. Barger, and J. A. C. Kaiser, "High-resolution measurement of surface-active film redistribution in ship wakes," *J. Geophys. Res.* **97**(C4), 5231–5252 (1992).
4. A. M. Reed, R. F. Beck, O. M. Griffin, and R. D. Peltzer, "Hydrodynamics of remotely sensed surface ship wakes," *Soc. Nav. Arch. Mar. Eng. Trans.* **98**, 319–363 (1990).
5. J. D. McGlynn, S. R. Stewart, and D. J. Witte, "Advances in sensing and detection of thermal infrared ship wakes," presented at Oceans' 90: Engineering in the Ocean Environment, Washington D.C., 1990, 24–26 September 1990.
6. W. H. Munk, P. Scully-Power, and F. Zachariassen, "Ships from space," *Proc. R. Soc. London Ser. A* **412**, 231–254 (1987).
7. X. Zhang, M. R. Lewis, and B. D. Johnson, "Influence of bubbles on scattering of light in the ocean," *Appl. Opt.* **37**, 6525–6536 (1998).
8. D. Stramski, "Gas microbubbles: an assessment of their significance to light scattering in quiescent seas," in *Ocean Optics XII*, J. S. Jaffe, ed., *Proc. SPIE* **2258**, 704–710 (1994).
9. D. Stramski and J. Tegowski, "Effects of intermittent entrainment of air bubbles by breaking wind waves on ocean reflectance and underwater light field," *J. Geophys. Res.* **106**(C12), 31345–31360 (2001).
10. A. Morel and L. Prieur, "Analysis of variations in ocean color," *Limnol. Oceanogr.* **22**, 709–722 (1977).
11. J. T. Tate and L. J. Spitzer, eds., *Physics of Sound in the Sea: Summary Technical Report of Division 6* (U.S. Government Printing Office, Washington D.C., 1946), p. 566.
12. M. V. Trevorrow, S. Vagle, and D. M. Farmer, "Acoustical measurements of microbubbles within ship wakes," *J. Acoust. Soc. Am.* **95**, 1922–1930 (1994).
13. L. Shen, C. Zhang, and D. K. P. Yue, "Free-surface turbulent wake behind towed ship models: Experimental measurements, stability analyses and direct numerical simulations," *J. Fluid Mech.* **469**, 89–120 (2002).
14. A. B. Ezerskii, B. M. Sandler, and D. A. Selivanovskii, "Echo-ranging observations of gas bubbles near the sea surface," *Sov. Phys. Acoust.* **35**, 483–485 (1989).

15. A. Morel and S. Maritorena, "Bio-optical properties of oceanic waters: A reappraisal," *J. Geophys. Res.* **106**(C4), 7163–7180 (2001).
16. A. Morel and J. L. Mueller, "Normalized water-leaving radiance and remote sensing reflectance: Bidirectional reflectance and other factors," in *Ocean Optics Protocols for Satellite Ocean Color Sensor Validation*, J. L. Mueller and G. S. Fargion, eds. (National Aeronautics and Space Administration, Greenbelt, Md., 2002), Revision 3, Vol. 2, p. 308.
17. H. R. Gordon, O. B. Brown, and M. M. Jacobs, "Computed relationships between the inherent and apparent optical properties of a flat homogeneous ocean," *Appl. Opt.* **14**, 417–427 (1975).
18. A. Morel and B. Gentili, "Diffuse reflectance of oceanic waters: Its dependence on sun angle as influenced by the molecular scattering contribution," *Appl. Opt.* **30**, 4427–4438 (1991).
19. A. Morel and B. Gentili, "Diffuse reflectance of oceanic waters. II. Bidirectional aspects," *Appl. Opt.* **32**, 6864–6879 (1993).
20. A. Morel, "Optical properties of pure water and pure sea water," in *Optical Aspects of Oceanography*, N. G. Jerlov and E. S. Nielsen, eds. (Academic, New York, 1974), pp. 1–24.
21. X. Zhang, "Influence of bubbles on the water-leaving reflectance," Ph.D. thesis (Dalhousie University, Halifax, Nova Scotia, Canada, 2001).
22. "LEO-15 Longterm Ecosystem Observatory" (Rutgers University, New Brunswick, N.J., 2001), retrieved March 2001, <http://marine.rutgers.edu/mrs/LEO15.html>.
23. R. W. Austin and T. L. Petzold, "The determination of the diffuse attenuation coefficient of sea water using the Coastal Zone Color Scanner," in *Oceanography from Space*, J. F. R. Gower, ed. (Plenum, New York, 1981), pp. 239–256.
24. A. Morel, "Optical modeling of the upper ocean in relation to its biogenous matter content (case I waters)," *J. Geophys. Res.* **93**(C9), 10749–10768 (1988).
25. B. D. Johnson and R. C. Cooke, "Bubble populations and spectra in coastal waters. A photographic approach," *J. Geophys. Res.* **84**, 3761–3766 (1979).
26. A. Berk, L. S. Bernstein, G. P. Anderson, P. K. Acharya, D. C. Robertson, J. H. Chetwynd, and S. M. Adler-Golden, "MODTRAN cloud and multiple scattering upgrades with application to AVIRIS," *Remote Sens. Environ.* **65**, 367–375 (1998).
27. H. R. Gordon, "Atmospheric correction of ocean color imagery in the Earth Observing System era," *J. Geophys. Res.* **102**(D14), 17081–17106 (1997).
28. C. D. Mobley, *Light and Water: Radiative Transfer in Natural Waters* (Academic, San Diego, Calif., 1994), p. 592.
29. A. Morel, "Light and marine photosynthesis: A spectral model with geochemical and climatological implications," *Prog. Oceanogr.* **26**, 263–306 (1991).
30. H. R. Gordon and A. Morel, *Remote Assessment of Ocean Color for Interpretation of Satellite Visible Imagery, a Review*, Vol. 4 of Springer-Verlag Lecture Notes on Coastal and Estuarine Studies Series (Springer-Verlag, New York, 1983), p. 114.
31. T. J. Petzold, "Volume scattering function for selected ocean waters," SIO Ref. 72–78 (Scripps Institute of Oceanography, La Jolla, Calif., 1972).
32. M. R. Lewis, J. J. Cullen, and T. Platt, "Phytoplankton and thermal structure in the upper ocean: consequences of non-uniformity in chlorophyll profile," *J. Geophys. Res.* **88**, 2565–2570 (1983).
33. X. Zhang, M. R. Lewis, M. Lee, B. D. Johnson, and G. Korotaev, "Volume scattering function of natural bubble populations," *Limnol. Oceanogr.* **47**, 1273–1282 (2002).
34. C. Garrett, M. Li, and D. M. Farmer, "The connection between bubble size spectra and energy dissipation rates in the upper ocean," *J. Phys. Oceanogr.* **30**, 2163–2171 (2000).
35. M. Y. Su, S. C. Ling, and J. Cartmill, "Optical microbubble measurements in the North Sea," in *Sea Surface Sound*, B. R. Kerman, ed. (Kluwer Academic, New York, 1988), pp. 211–223.
36. E. J. Terrill, W. K. Melville, and D. Stramski, "Bubble entrainment by breaking waves and their influence on optical scattering in the upper ocean," *J. Geophys. Res.* **106**(C8), 16815–16823 (2001).
37. D. J. Bogucki, J. A. Domaradzki, D. Stramski, and J. R. V. Zaneveld, "Comparison of near-forward light scattering on oceanic turbulence and particles," *Appl. Opt.* **37**, 4669–4677 (1998).
38. R. Frouin, M. Schwindling, and P.-Y. Deschamps, "Spectral reflectance of sea foam in the visible and near-infrared: *in situ* measurements and remote sensing implications," *J. Geophys. Res.* **101**(C6), 14361–14371 (1996).
39. H. R. Gordon, "Sensitivity of radiative transfer to small-angle scattering in the ocean: quantitative assessment," *Appl. Opt.* **32**, 7505–7511 (1993).
40. C. D. Mobley, "Estimation of the remote-sensing reflectance from above-surface measurements," *Appl. Opt.* **38**(36), 7442–7455 (1999).
41. M. Viollier, D. Tanré, and P. Y. Deschamps, "An algorithm for remote sensing of water color from space," *Boundary-Layer Meteorol.* **18**, 247–267 (1980).
42. C. Cox and W. Munk, "Statistics of the sea surface derived from sun glitter," *J. Mar. Res.* **13**, 198–227 (1954).
43. C. H. Whitlock, D. S. Bartlett, and E. A. Gurganus, "Sea foam reflectance and influence on optimum wavelength for remote sensing of ocean aerosols," *Geophys. Res. Lett.* **9**, 719–722 (1982).
44. P. Koepke, "Effective reflectance of oceanic whitecaps," *Appl. Opt.* **23**, 1816–1824 (1984).
45. K. D. Moore, K. J. Voss, and H. R. Gordon, "Spectral reflectance of whitecaps: their contribution to water-leaving radiance," *J. Geophys. Res.* **105**(C3), 6493–6499 (2000).
46. H. R. Gordon and M. Wang, "Retrieval of water-leaving radiance and aerosol optical thickness over the oceans with SeaWiFS: A preliminary algorithm," *Appl. Opt.* **33**(3), 443–452 (1994).